19th Australasian Fluid Mechanics Conference
Melbourne, Australia
8-11 December 2014

A Numerical and Experimental Study on the Unsteady Conjugate Natural Convection Boundary Layers in a Water Filled Rectangular Cavity with a Conducting Partition Wall at Varied Locations

M. Khatamifar[1], R. D'Urso[1], W. Lin[1,2], D. Holmes[1], S. W. Armfield[3] and M. P. Kirkpatrick[3]

[1]College of Science, Technology & Engineering
James Cook University, Townsville, QLD 4811, Australia

[2]Solar Energy Research Institute
Yunnan Normal University, Kunming, Yunnan 650092, China

[2]School of Aerospace, Mechanical and Mechatronic Engineering
The University of Sydney, NSW 2006, Australia

Abstract

This paper presents some preliminary results on the behavior of unsteady conjugate natural convection boundary layers (CNCBLs) in a water filled rectangular cavity with a partition wall at varied locations through a series of experiments and two-dimensional direct numerical simulations (DNS). The experiments were carried out over $2.428 \times 10^9 \leq Ra \leq 2.458 \times 10^{10}$ and $5.3701 \leq Pr \leq 6.1697$, with the partition wall placed at the center of the cavity, where *Ra* and *Pr* are the Rayleigh and Prandtl numbers, respectively. The temperatures at eight locations in the cavity were measured by Resistance Temperature Detectors (RTDs). The DNS runs were carried out using a code developed in house based on the finite-difference method and written in Visual C#.NET programming language. The DNS runs complement and expand the experiments by providing additional information about the behavior of unsteady CNCBLs and the effects of the variation of the partition position.

Introduction

Heat transfer between two fluid reservoirs at different temperatures through a vertical separating conducting wall occurs widely in nature and engineering applications. The phenomenon is particularly important in power plants, polymer production, chemical reactors, food processing, computer and electronic instruments design, building design, and geophysical flows, in addition to its fundamental significance. The heat transfer in such a configuration is via a mechanism called conjugate natural convection boundary layers (CNCBLs). On the side of the partition wall contacting with the fluid at a higher temperature, a natural convection boundary layer forms and moves down along the wall whereas on the other side of the wall which is in contact with the fluid at a lower temperature, a similar boundary layer forms and moves up along the wall, both due to the buoyancy caused by the temperature difference between the wall and the fluid in contact. Heat are transferred through the conducting partition wall, from the fluid at a higher temperature to the fluid at a lower temperature. As the partition wall temperature changes with the development of the CNCBLs, it becomes part of the solution of the flow and heat transfer, which makes the prediction of the behaviour of the flow and heat transfer in such a configuration complicated and hard.

There have been many studies on CNCBLs, with the majority dealing only with their steady behavior (see, e.g., [1, 2, 3]). The behavior of unsteady CNCBLs is still poorly understood, which motivates this study, where both physical experiments and two-dimensional DNS simulations are carried out to examine the behavior of unsteady CNCBLs in a water filled rectangular cavity with a conducting partition wall at varied locations.

Methodologies

Experimental Methods

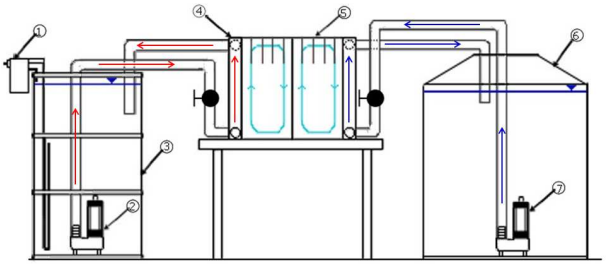

Figure 1. Schematic of the experimental setup: 1. OTS heater (240V 5000W), 2. Davey D40VA sump pump, 3. 205 L galvanized steel drum with water at temperature higher than the ambient, 4. Experimental tank ($400 \times 400 \times 600$ mm, Perspex front and rear, PVC top and bottom, 3 mm aluminum alloy 5083 partition plate and side heat exchangers), 5. 8×Resistance temperature detectors (RTDs), 6. 1000 L plastic tank with water at ambient temperature, 7. Davey D15VA sump pump.

The experimental setup is sketched in figure 1. The rectangular experimental tank was of the dimensions 400 mm × 400 mm × 600 mm ($L \times W \times H$). It had Perspex front and rear sides, and PVC top and bottom sides. Its left and right vertical sides were two aluminium heat exchangers, which, by circulating hot/cold water through them from the hot/cold water reservoirs respectively, produced and maintained a constant but different temperature (T_h and T_c for hot and cold water) on each side during the course of each experiment run. The tank was insulated by 50 mm thick polystyrene foam sheets at the top, bottom, rear and front sides, which made it appropriate to assume that the heat transferred across these four sides is negligible. A galvanized 205 L drum and a 1000 L plastic tank were used as the hot/cold water reservoirs, respectively. In each of these tanks, a submersible sump pump was placed to pump hot/cold water through the aluminium heat exchangers. The Davey D40VA/D15VA sump pump used for the hot/cold water reservoir pumped hot/cold water at a flow rate of approximately 189/131 L/min. The use of such large flow rates was to ensure that the inside wall of each heat exchanger was maintained at a constant temperature. A 3 mm aluminum alloy 5083 partition wall with a thermal conductivity of $\kappa_p \approx 121$ W/m-K was centrally positioned in the tank (*i.e.*, x_p=0.5, where x_p is the partition position ratio with respect to the cavity length), which divides the tank into two separate but equal-sized domains.

To examine the evolution of the temperatures in the cavity, eight

calibrated PT100 RTD probes were inserted through the holes at predetermined locations on the top surface of the experimental tank. The RTDs were in the central plane of the tank in the spanwise direction and 75 mm below the top surface. Their locations were 20 mm, 75 mm, 130 mm, 185 mm, 215 mm, 270 mm, 325 mm, and 380 mm away from the left vertical sidewall, respectively, for the RTDs numbered from 1 to 8. The RTDs were connected to a DT85 dataTaker Data Logger that recorded the temperatures measured by the probes at 1-second intervals. This frequency of logging was found to give an ideal resolution on the temperature evolution. The temperature of the hot water tank was controlled by a 5000W digital temperature controlled immersion heater. This contained a built-in AC1-5P LAE electronic controller and a PT100 RTD that allowed for accurate (± 0.3 ^{o}C) PID heater control. The temperature of the cold water tank was at the room temperature and a PT100 RTD was inserted into the tank to measure it.

The flow is governed mainly by the dimensionless parameters Ra, Pr, A, x_p, and κ_r, where Ra and Pr are the Rayleigh and Prandtl numbers, A is the aspect ratio of the tank, and κ_r is the ratio of the thermal conductivity of the partition wall (κ_p) and that of water (κ_w), respectively, which are defined as,

$$Ra = \frac{g\beta_w(T_h - T_c)H^3}{\nu_w \alpha_w},\ Pr = \frac{\nu_w}{\alpha_w},\ A = \frac{L}{H},\ \kappa_r = \frac{\kappa_p}{\kappa_w}, \quad (1)$$

in which g is the acceleration due to gravity, β_w, ν_w and α_w are the thermal expansion coefficient, kinematic viscosity and thermal diffusivity of the fluid (water), respectively. $\alpha_w = \kappa_w/(\rho_w C_p)$, where ρ_w and C_p(=4180 kJ/kg-K) are the density and specific heat of water, and $\kappa_w \approx 0.6$ W/m-K.

Run	T_h (^{o}C)	T_c (^{o}C)	Ra	Pr
1	25.7	23.7	2.428×10^9	6.1697
2	26.1	23.1	3.621×10^9	6.1855
3	26.9	22.9	4.913×10^9	6.1381
4	28.6	23.6	6.582×10^9	5.9485
5	30.5	23.5	9.689×10^9	5.8111
6	32.5	23.5	1.308×10^{10}	5.6851
7	34.5	23.5	1.678×10^{10}	5.5591
8	37.0	24.0	2.130×10^{10}	5.3701
9	38.0	23.0	2.458×10^{10}	5.3701

Table 1. Details of the experimental runs.

Totally nine experiment runs were carried out, over $2.428 \times 10^9 \le Ra \le 2.458 \times 10^{10}$ and $5.3701 \le Pr \le 6.1697$, all at $A = 1$, $x_p = 0.5$ and $\kappa_r \approx 202$. All these experiments were conducted with the same tank and partition configuration and the variations of Ra and Pr were achieved by changing the hot water temperature through the OTS heater. The details about these experimental runs are listed in table 1.

Numerical Methods

With the experiments, the scope of this study is quite limited as only measured temperatures at eight fixed locations in the cavity can be provided by the experiments due to the experimental setup. In addition, only one specific water tank and partition configuration is used in the experiments. A series of two-dimensional DNS runs are therefore carried out to complement and expand the experiments, which provide additional detailed information about the behavior of unsteady CNCBLs, such as the temperature and velocity fields, thermal and viscous boundary layer thicknesses, Nusselt number, etc. Furthermore, with the DNS runs, the behavior of unsteady CNCBLs at varied partition positions and different configurations can be examined.

The governing equations for DNS are the continuity, Navier-Stokes, and temperature equations for the fluid in the cavity and the heat conduction equation in the partition wall. With the Oberbeck-Boussinesq approximation for buoyancy, these equations can be written in dimensionless forms as follows,

$$\frac{\partial u}{\partial x} + \frac{\partial v}{\partial y} = 0, \quad (2)$$

$$\frac{\partial u}{\partial \tau} + u\frac{\partial u}{\partial x} + v\frac{\partial u}{\partial y} = -\frac{\partial p}{\partial x} + \sqrt{\frac{Pr}{Ra}}\left(\frac{\partial^2 u}{\partial x^2} + \frac{\partial^2 u}{\partial y^2}\right), \quad (3)$$

$$\frac{\partial v}{\partial \tau} + u\frac{\partial v}{\partial x} + v\frac{\partial v}{\partial y} = -\frac{\partial p}{\partial y} + \sqrt{\frac{Pr}{Ra}}\left(\frac{\partial^2 v}{\partial x^2} + \frac{\partial^2 v}{\partial y^2}\right) + \theta, \quad (4)$$

$$\frac{\partial \theta}{\partial \tau} + u\frac{\partial \theta}{\partial x} + v\frac{\partial \theta}{\partial y} = \sqrt{\frac{1}{PrRa}}\left(\frac{\partial^2 \theta}{\partial x^2} + \frac{\partial^2 \theta}{\partial y^2}\right), \quad (5)$$

$$\frac{\partial \theta}{\partial \tau} = \sqrt{\frac{\kappa_r}{PrRa}}\left(\frac{\partial^2 \theta}{\partial x^2} + \frac{\partial^2 \theta}{\partial y^2}\right), \quad (6)$$

where u and v are velocity components in the x and y directions, p is pressure, θ is temperature, and τ is time, which are made dimensionless by their respective characteristic scales, *i.e.*,

$$\left.\begin{aligned} x = \frac{X}{H},\quad y = \frac{Y}{H},\quad u = \frac{U}{V_0},\quad v = \frac{V}{V_0},\\ p = \frac{P}{\rho V_0^2},\quad \tau = \frac{t}{H/V_0},\quad \theta = \frac{T - T_0}{T_h - T_c}, \end{aligned}\right\} \quad (7)$$

in which U, V, X, Y, P, T, and t are the dimensional counterparts of u, v, x, y, p, θ, and τ, respectively. $V_0 = \sqrt{g\beta(T_h - T_c)}$ is used as the characteristic velocity scale. $T_0 = (T_h + T_c)/2$ is used as the reference temperature.

The initial conditions (when $\tau = 0$) are,

$$u = v = 0,\ \theta = -0.5 \text{ at all } x \text{ and } y, \quad (8)$$

and when $\tau > 0$ the boundary conditions for the fluid are,

$$\left.\begin{aligned} u = v = 0,\ \theta = 0.5 \text{ at } x = 0,\ 0 \le y \le 1,\\ u = v = 0,\ \theta = -0.5 \text{ at } x = A,\ 0 \le y \le 1,\\ u = v = 0,\ \frac{\partial \theta}{\partial y} = 0 \text{ at } y = 0,\ 0 \le x \le A,\\ u = v = 0,\ \frac{\partial \theta}{\partial y} = 0 \text{ at } y = 1,\ 0 \le x \le A, \end{aligned}\right\} \quad (9)$$

and for the partition wall the boundary conditions are,

$$\left.\begin{aligned} u = v = 0,\ \kappa_w \left.\frac{\partial \theta}{\partial y}\right|_{x_1^-} = \kappa_p \left.\frac{\partial \theta}{\partial y}\right|_{x_1^+} \text{ at } x = x_1,\ 0 \le y \le 1,\\ u = v = 0,\ \kappa_w \left.\frac{\partial \theta}{\partial y}\right|_{x_2^-} = \kappa_p \left.\frac{\partial \theta}{\partial y}\right|_{x_2^+} \text{ at } x = x_2,\ 0 \le y \le 1, \end{aligned}\right\} \quad (10)$$

where x_1 and x_2 are the locations of the left and right sides of the partition wall and the associated superscripts '-' and '+' denote their nearest left and right cells, respectively.

A DNS code based on the finite difference method and written in Visual C# .NET programming language was developed in house. The governing equations were discretised with a combination of explicit and implicit schemes. The SIMPLE algorithm was used to solve the coupled pressure and velocity. The method introduced by [4], in which ghost nodes at the fluid-solid interface are employed and the cavity flow and partition conduction are solved simultaneously, was used to deal with the conjugate flow and heat transfer at the partition wall. As

a staggered non-uniform mesh with 500×500 grids was used, some modifications were made to the method. The code has the explicit and implicit sections of calculation, with the explicit section calculating velocities and temperature for all cells and the implicit section consisting of a loop that calculates the continuity equation until convergence is attained. The velocities and temperatures are then updated and stored in the cells for the next time-step calculations.

Results

Time Series of Temperatures

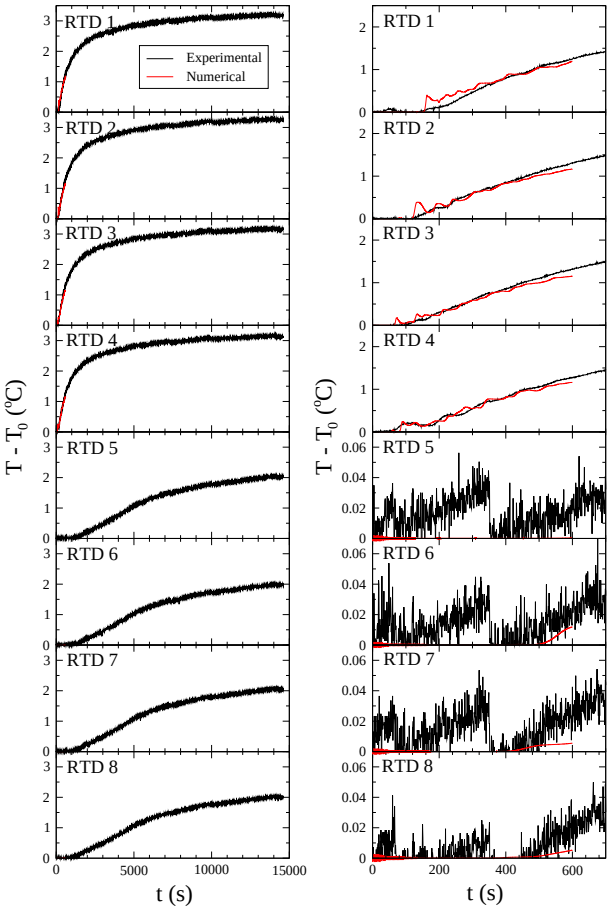

Figure 2. Time series of temperature $(T - T_0)$ at the eight points measured by the RTDs and obtained by the DNS runs, with the left and right columns for the whole durations and early stages of the measurements and simulations, respectively.

The time series of the temperatures at the eight points measured by the RTDs and obtained by the DNS runs for the representative case corresponding to the experiment run 2 are presented in figure 2. The results show that in the left domain the temperatures rise quickly at the early development stage but then approach to T_h very slowly and asymptotically, whereas the temperatures in the right domain rise in a significantly slower rate but also approach a final temperature slowly and asymptotically. For the case presented in the figure, the final temperature attained in the right domain is about 2/3 of T_h at the end of the experiment and DNS run, apparently due to the conjugate heat transfer on the partition wall. Theoretically it is expected that the temperatures in both domains will attain T_h if the heating applied on the left vertical side lasts infinitely.

The DNS results obtained so far only cover the early development stage due to the extensive computation requirements. The comparison with the experimental results shows that the DNS results are in general in good agreement with the experimental results, although noticeable deviations are observed during the course of the passage of first intrusion through these measurement points. The deviations are most likely caused by the mesh used which may not be fine enough to resolve the smallest scales as the flow, at $Ra = 3.621 \times 10^9$, is at the transition to turbulent regimes. A finer mesh is expected to significantly reduce the deviations and the results will be reported at the conference. Another possible cause may come from the two-dimensional flow assumption in the DNS as at such a high Ra, the flow should be three-dimensional.

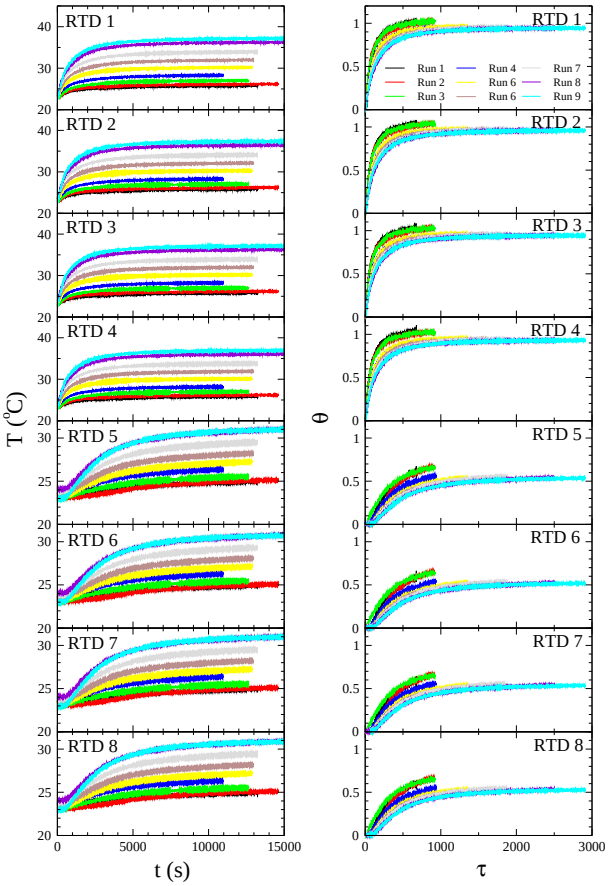

Figure 3. Time series of dimensional temperatures T (left column) and dimensionless temperatures θ (right column) at the eight points measured by the RTDs for all 9 experimental runs.

The time series of the measured temperatures at the 8 RTDS for all 9 experiment runs are presented in figure 3. The general behavior observed from figure 2 for the experiment run 2 is also observed for all other 8 experiment runs. It is interesting to note that when $T_h - T_c$ increases, the temperatures at the 4 RTDs in the right domain approach an eventual dimensionless temperature, again asymptotically, which is smaller than that for a smaller $T_h - T_c$. This may be caused by the increasing heat loss through the insulation when $T_h - T_c$ increases. But some further studies should be carried out to examine this.

Evolution of Temperature Fields

The evolution of temperature fields obtained by DNS is presented, as an example, in figure 4 for $Ra = 3.621 \times 10^9$, $Pr = 6.1855$, $A = 1$, and $\kappa_r = 202$, but at x_p=0.3, 0.5, and 0.7, respectively. The effect of x_p on the stratification of fluids in the left and right domains is obvious; the stratification in the left domain develops quicker for smaller x_p but that in the right do-

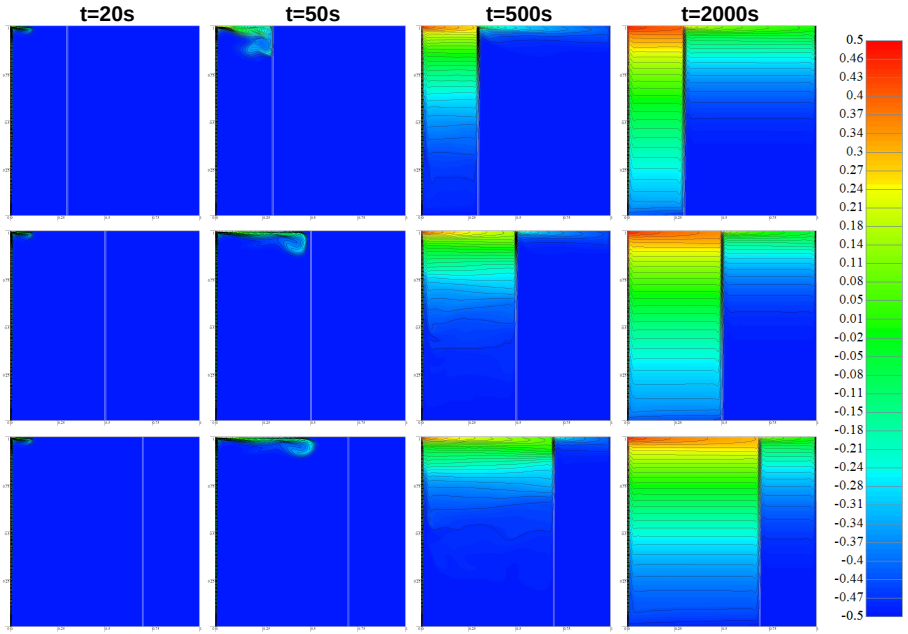

Figure 4. Temperature contours at four times for $x_p = 0.3$ (first row), 0.5 (second row), and 0.7 (third row), respectively.

main is just the opposite, due to smaller heat transfer rate across the partition wall. It is expected that the fluid in the left domain will attain T_h faster for smaller x_p but that in the right domain will take much longer time to attain its asymptotic temperature.

Horizontal Profiles of θ and *v*

Figure 5 presents the evolution of the horizontal profiles of θ and v at $y = 0.5$ obtained by DNS for the case of $Ra = 3.621 \times 10^9$, $Pr = 6.1855$, $A = 1$, $\kappa_r = 202$, and x_p=0.5. The formation and development of boundary layers on the left and right vertical sides and the CNCBLs on the both sides of the partition wall are clearly shown and in the middle regions of both domains, stratification is well developed at the later stage.

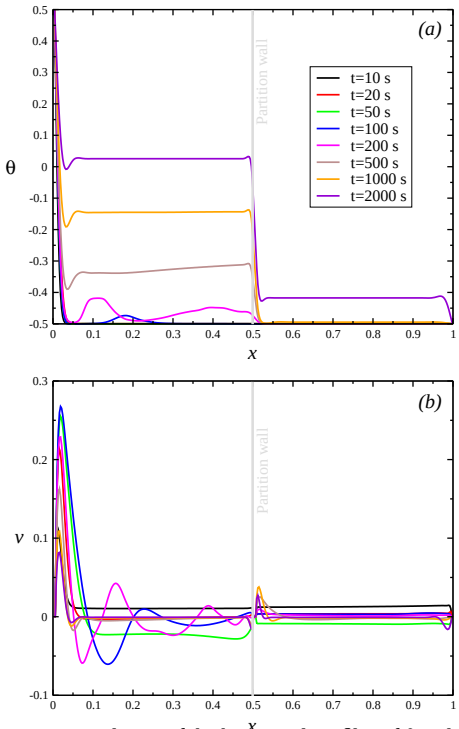

Figure 5. Evolution of the horizontal profiles of θ and *v*.

Conclusions

In this paper, some preliminary results obtained experimentally and numerically are presented to show the behavior of unsteady CNCBLs with varied partition locations. The two-dimensional DNS results, which were obtained by using a code specifically developed in house based on the finite-difference method and written in Visual C#.NET programming language, are found in general to be in good agreement with the experimental results, but they complement and expand the experiments by providing additional information about the behavior of unsteady CNCBLs and the effects of the variation of the partition position. More detailed results will be presented at the conference.

Acknowledgements

The support from the Australian Research Council (ARC), the National Natural Science Foundation of China (51469035, 11072211), and the Yunnan Natural Science Foundation (2011FA017) is gratefully acknowledged. M. Khatamifar also thanks James Cook University for the JCUPRS scholarship.

References

[1] Lock, G.S.H. and Ko, R.S., Coupling Throught a Wall Between Two Free Convective Systems, *Int. J. Heat Mass Transfer*, **16**, 1973, 2087–2096.

[2] Xu, F., Patterson, J.C. and Lei, C., Heat Transfer Through Coupled Thermal Boundary Layers Induced by a Suddenly Generated Temperature Difference, *Int. J. Heat Mass Transfer*, **52**, 2009, 4966–4975.

[3] Williamson, N., Armfield, S.W. and Kirkpatrick, M.P., Transition to Oscillatory Flow in a Differentially Heated Cavity with a Conducting Partition, *J. Fluid Mech.*, **693**, 2012, 93–114.

[4] Carlson, K.D., Lin, W. and Chen, C.-J., Pressure Boundary Conditions of Incompressible Flows with Conjugate Heat Transfer on Nonstaggered Grids. Part ii: Applications, *Numerical Heat Transfer, Part A: Applications*, **32**, 1997, 481–501.